HAIT Journal of Science and Engineering B, Volume 2, Issue 5-6, pp. 638-654

Buck converter digitally controlled by a fuzzy state-space controller

Miro Milanovič* and Dušan Gleich

[1] *Faculty of Electrical Engineering and Computer Science, University of Maribor, Maribor, Slovenia*
* *Corresponding author: milanovic@uni-mb.si*

Received 1 March 2005, accepted 10 November 2005

Abstract

In this paper a digitally controlled step down converter using fuzzy state space controller is studied. The state controller is designed to eliminate the start-up overshoot and reduce maximal dynamic error of load change response, but the state controller is not capable to eliminate the steady-state error under the load change condition. In order to improve this property, two control algorithms were investigated. The first one was the state controller with constant gains supported by an additional decomposed fuzzy PID controller and the second one was a fuzzy state space controller. Both of control algorithms are performed at a continuous current mode of operation. The experimental results are presented in the paper. The control algorithms are implemented on 16-bit DSP unit. All algorithm are suitable for implementation by FPGA as well.

1 Introduction

DC-DC converters are nonlinear systems due to their inherent switching operation. To assure a constant output voltage, a classical linear design of a control is frequently used. The regulation is normally achieved by the pulse width modulation (PWM) at a fixed frequency. The switching device is a power MOSFET. The PWM linear control techniques are widely used [1]. Sliding-mode control based techniques [2] exhibit the property of

robustness in front of large signal perturbations, leading to global stability. The sliding controller parameters lead to an optimal behaviour in large signal operation and do not yield an optimal small-signal behaviour. During the last decade, digital control in power electronics has been intensively used. The increasing performance and cost reduction of digital circuits has enabled their application for power converters control. The control algorithms are implemented on digital signal processors (DSP), which are not very common in high switching frequency domain or low cost applications. Some control algorithms are implemented in the field of programmable gate array (FPGA) using hardware description language (VHDL) [3].

An ordinary state control algorithm and two control structures based on the fuzzy-set approach are presented in this paper. The fuzzy-set theory has evolved as a powerful modeling tool that can cope with the uncertainties and non-linearity of the control systems [4, 5]. The first algorithm considered in this paper is based on state controller. In the second case, the state controller was supported by decomposed fuzzy PID controller in order to eliminate the static error and to improve the converter dynamics. The PID controller gains were adjusted by the fuzzy-set approach. The third one is a fuzzy state controller, where a nonlinear fuzzy approach is used for adaptive state controller gain adjustment in order to minimize the steady state error and improve dynamics. During the experimental works, it was simple to change the controller structure without any external passive or active components. The control law is programmable so it is easy to implement different control algorithms. Both algorithms were verified by experiment.

2 DSP implemented controllers

In Fig. 1 the DSP controlled buck converter is shown. The state controller and two control structures based on the fuzzy-set approach were investigated. Disadvantages as large settling time and steady state-error were recognized at ordinary state controller. Due to this, two fuzzy-set controllers were discussed: decomposed fuzzy PID controller with ordinary state controller and fuzzy state space controller. In outer control loop the PID control law was introduced. The PID controller gains were adapted by the fuzzy rules. A second fuzzy algorithm was used to adjust the state controller gains.

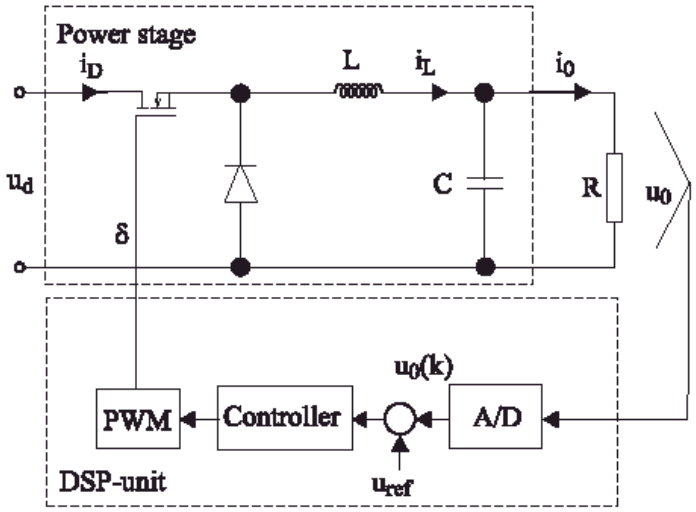

Figure 1: DSP based control scheme.

2.1 The state control of the buck converter

The buck converter is modeled using an averaged signal model [1]. From the power stage part in Fig. 1, a buck converter model is obtained using linear differential equations:

$$\begin{bmatrix} \frac{di_L}{dt} \\ \frac{du_0}{dt} \end{bmatrix} = \begin{bmatrix} -\frac{R_L}{L} & -\frac{1}{L} \\ \frac{1}{C} & -\frac{1}{RC} \end{bmatrix} \begin{bmatrix} i_L \\ u_0 \end{bmatrix} + \begin{bmatrix} \frac{1}{L} \\ 0 \end{bmatrix} u_d\delta \tag{1}$$

where i_L is the inductor current, u_0 is the output voltage, u_d is the input voltage, δ is the duty cycle, L is the circuit inductance, R_L is the resistance of inductor, C is the output capacitance, and R is the load resistance. In order to get a dynamic model, the small signal perturbation must be introduced:

$$\begin{aligned} u_d &= U_d + \tilde{u}_d \\ u_C &= U_C + \tilde{u}_C \\ i_C &= I_C + \tilde{i}_C \\ \delta &= \Delta + \tilde{\delta} \end{aligned}$$

where capital letters are used to describe the converter operating point and represent the average values of variables. The corresponding transfer func-

tion of the continuous system is given by:

$$H_1(s) = \frac{\tilde{u}_0(s)}{\tilde{\delta}(s)}\Big|_{\tilde{u}_d=0} = \frac{U_d}{as^2 + bs + c} \tag{2}$$

with

$$\begin{aligned} a &= LC, \\ b &= \frac{L}{R} + R_L C \\ c &= 1 + \frac{R_L}{R} \end{aligned}$$

where $R = 6.8\ \Omega$, $L = 2.1\text{mH}$, $C = 100\ \mu\text{F}$, $R_L = 1.1\ \Omega$, and $U_d = 12\text{V}$ have been chosen. In order to control the state variables, the output voltage u_0 and its derivative du_0/dt were chosen. For this purposes, a controllable canonical form is obtained from (2) (Fig. 2):

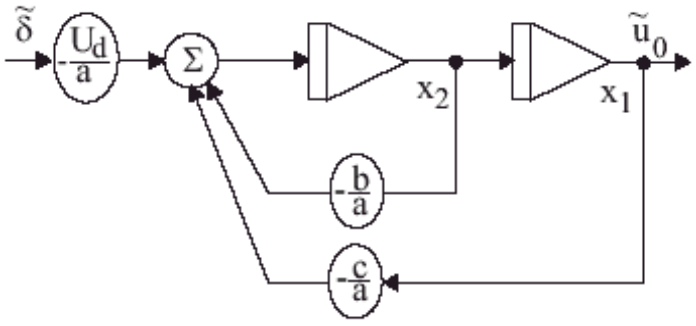

Figure 2: Canonical form of converter model.

$$\begin{aligned} \begin{bmatrix} \frac{d\tilde{x}_1}{dt} \\ \frac{d\tilde{x}_2}{dt} \end{bmatrix} &= \begin{bmatrix} 0 & 1 \\ -\frac{c}{a} & -\frac{b}{a} \end{bmatrix} \begin{bmatrix} \tilde{x}_1 \\ \tilde{x}_2 \end{bmatrix} + \begin{bmatrix} 0 \\ \frac{U_d}{a} \end{bmatrix} \tilde{\delta} \\ \begin{bmatrix} \tilde{y}_1 \\ \tilde{y}_2 \end{bmatrix} &= \begin{bmatrix} \tilde{u}_0 \\ \tilde{du}_0/dt \end{bmatrix} = \begin{bmatrix} 1 & 0 \end{bmatrix} \begin{bmatrix} \tilde{x}_1 \\ \tilde{x}_2 \end{bmatrix} \end{aligned} \tag{3}$$

where $x_1 = u_0$ and $x_2 = \frac{du_0}{dt}$. The obtained model is verified by experimental results shown in Fig. 3. The load resistance R changed from 6.8 Ω to 4.8 Ω

and duty cycle δ was 0.42. The above system could be written in a matrix form:

$$\begin{aligned} \frac{d\tilde{\mathbf{x}}(t)}{dt} &= \mathbf{A}\tilde{\mathbf{x}}(t) + \mathbf{B}\tilde{u}(t) \\ \tilde{\mathbf{y}}(t) &= \mathbf{C}\tilde{\mathbf{x}}(t). \end{aligned} \tag{4}$$

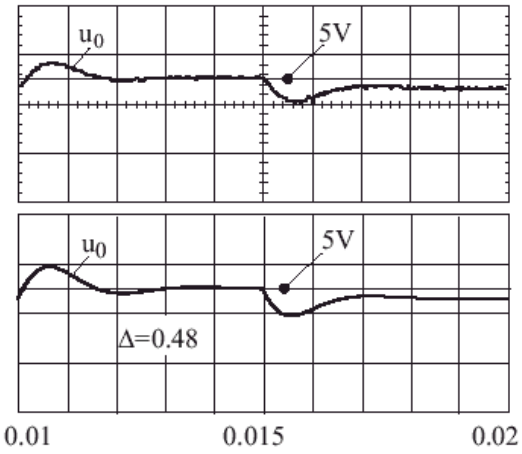

Figure 3: The model verification, the experimental results (above), and the simulation results.

The continuous system is discretized by using a sample time which guarantees the fulfillment of the Nyquist criteria. The sampling rate was chosen as $f_s \geq 1/(2\pi\sqrt{LC})$. The switching frequency of PWM and sampling time in all presented experiments was $T_s = 50$ μs. The discretized system is:

$$\begin{aligned} \tilde{\mathbf{x}}(k+1) &= \mathbf{\Phi}\tilde{\mathbf{x}}(k) + \mathbf{\Gamma}\tilde{u}(k) \\ \tilde{\mathbf{y}}(k) &= \mathbf{C}\tilde{\mathbf{x}}(k). \end{aligned} \tag{5}$$

After discretization of (4), the discrete matrices $\mathbf{\Phi}$ and Γ were evaluated:

$$\begin{aligned} \mathbf{\Phi} &= \begin{bmatrix} +5.54 \times 10^{-1} & +1.19 \times 10^{-6} \\ -6.84 \times 10^{+3} & -1.47 \times 10^{-2} \end{bmatrix} \\ \mathbf{\Gamma} &= \begin{bmatrix} 0.43 \\ 6.79 \times 10^{4} \end{bmatrix} \\ \mathbf{C} &= \begin{bmatrix} 1 & 0 \end{bmatrix}. \end{aligned}$$

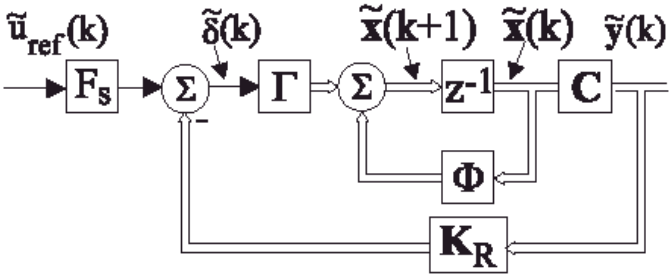

Figure 4: The state controller scheme.

The control scheme is shown in Fig. 4. The state controller was determined using a standard approach. The poles of the system were chosen in such a way that the damping factor $D = 1$ and the frequency $\omega_0 = 8000$ for the characteristic polinomial $s^2 + 2d\omega_0 + \omega_0^2$ in the continuous space. The parameters were transformed into a discrete space, and poles of the closed loop discrete transfer function were evaluated as $z_1 = z_2 = e^{-d\omega_0 T} = 0.637$. According to this, the discrete state controller gains are:

$$\mathbf{K}_R = \left[\begin{array}{cc} K_{r1} & K_{r2} \end{array} \right] = \left[\begin{array}{cc} -7.19 \times 10^{-2} & -6.13 \times 10^{-6} \end{array} \right]. \tag{6}$$

According to (5) and (6), the closed loop discrete transfer function is:

$$H_2(z) = \frac{\tilde{u}_0}{\tilde{u}_{ref}} = \frac{0.023z + 0.02}{z^2 - 1.81z + 0.82}. \tag{7}$$

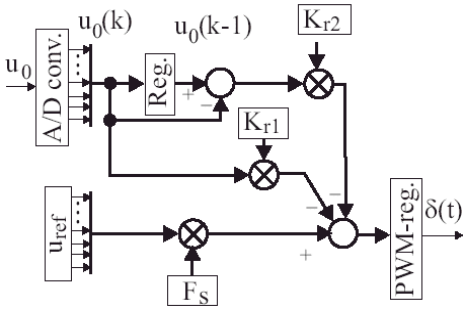

Figure 5: The state controller scheme (DSP implementation).

In order to reduce the steady state, the static gain was introduced. The gain has been evaluated by:

$$F_S = \frac{1}{\lim_{z\to 1} H_2(z)} = 34.7.$$

Fig. 5 shown the structure of state controller. The controller was implemented on the 16-bit microcomputer. The A/D converter and timer (PWM) were used as necessary peripheral units. The voltage $u_0(k)$ was measured. The voltage derivative was replaced by the finite difference ($u_{diff.}(k) = u_0(k) - u_0(k-1)$). The reference (output) voltage was set to $u_{ref} = (u_0) =$ 3.3V. The start-up of the state-space controlled converter and the transient

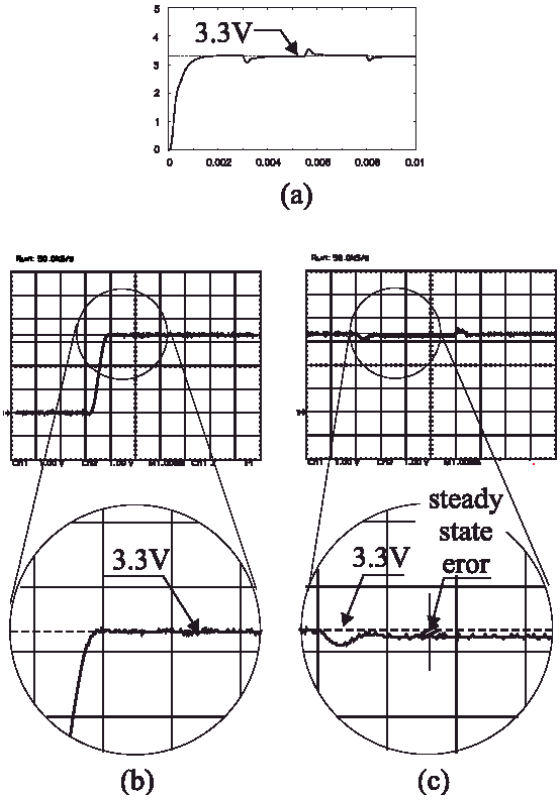

Figure 6: The state space controller response. (a) Matlab-Simulink simulation of state controlled buck converter, start-up and load change response; experimental start-up (b) and load charge (c) response ($R = 6.8$ to 4.8 Ω).

response after the load resistance are shown in Fig. 6a,b, and c, respectively. The control algorithm is investigated by simulation as shown in Fig. 6a and than by experiment shown in Fig. 6b and 6c. There is no overshoot at the start-up, but the steady state error is noticed when the load resistance is changed. The voltage overshoot at the load change is 510 mV peak-to-peak (Vpp) and the steady state error is around 78 mV. The settling time of the step response was 1ms and the settling time at the load resistance change was 800μs. The steady state error could be diminished by introducing the additional voltage control loop with PID controller supported by fuzzy algorithm, as shown in Fig. 7.

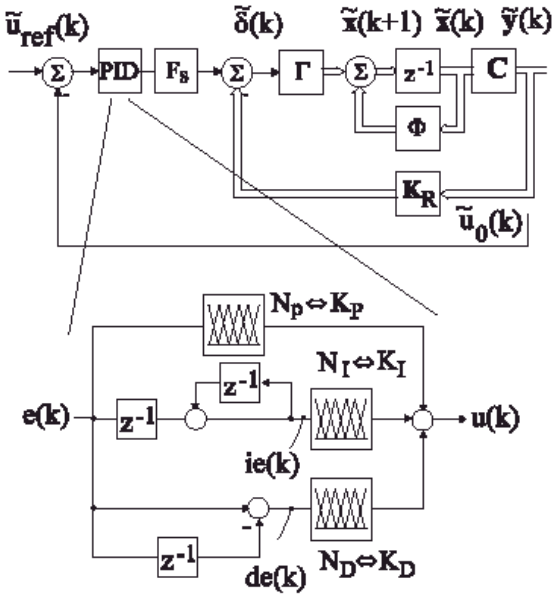

Figure 7: The decomposed PID fuzzy controller scheme.

2.2 Decomposed fuzzy PID controller

Better dynamic response and lower steady state error of the converter can be reached by introducing the decomposed fuzzy PID controller. These properties can be improved by adaptation of the PID controller constants K_p, K_i, and K_d . It is obvious that the parameters denoted by b and c in (2) will change the buck converter dynamics under the load change condition.

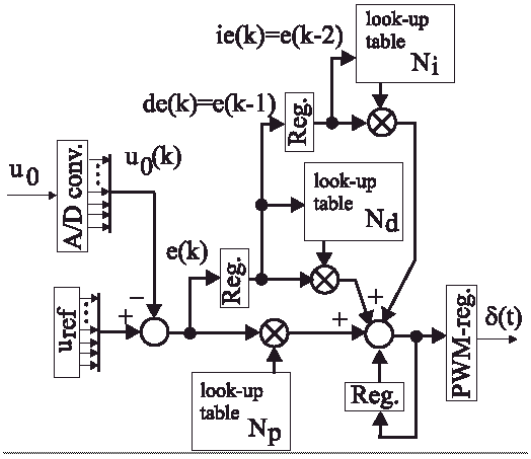

Figure 8: The decomposed fuzzy PID controller (DSP implementation).

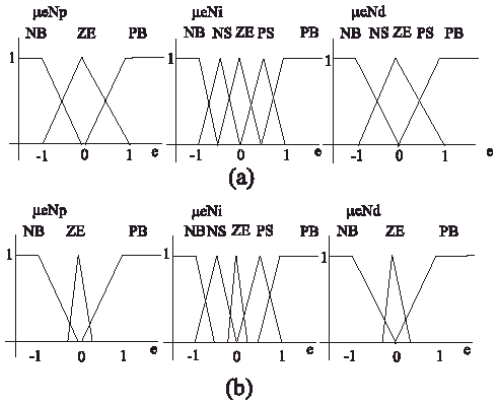

Figure 9: Membership functions of a PID controller: (a) input membership function, (b) output membership function.

Due to this, the decomposed fuzzy PID controller can be used [5]. The output of the fuzzy PID controller is denoted by:

$$u(k) = N_p(e(k)) + N_D(de(k)) + N_I(ie(k)) \tag{8}$$

where N_P, N_D, and N_I are the non-linear functions determined by a Fuzzy Rule-Based System (FRBS). A FRBS presents two main components: the

Rule Base (RB), representing the knowledge about the controller and described in the form of the fuzzy IF-THEN rules, and the Fuzzy Inference System (FIS) needed to obtain an output from FRBS. The structure of the fuzzy PID controller is depicted in Fig. 7.

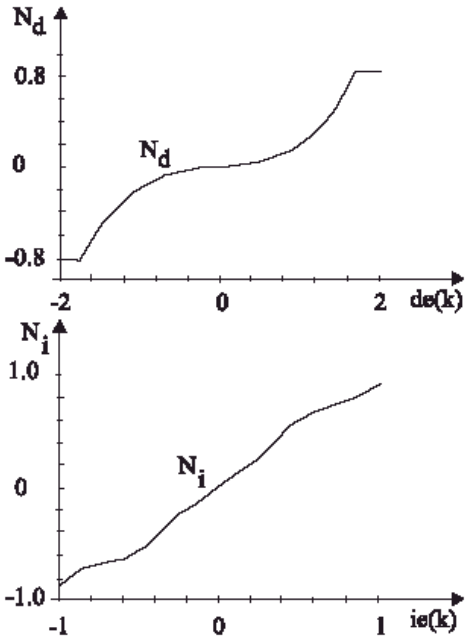

Figure 10: The K_p, K_i, and K_d non-linearity.

The linguistic description of the knowledge base is given by three RB's. The output signal is the sum of the defuzzified outputs of proportional FIS, differential FIS, and integral FIS. The proportional part will produce linear effect and the integral and differential parts will produce the non-linear effect. The membership functions are shown in Fig. 9. The fuzzy rules were designed in such a way that for each input membership function the output membership function was assigned. In Table 1, five fuzzy rules for the linguistic variable N_i are shown. Similar fuzzy rules were assigned to the integral and differential parts. For variables N_p and N_d, only 3 fuzzy rules (1), (3), and (5) were used.

The non-linearity of PID controller gains are designed by using the FRBS shown in Fig. 9 and linguistic description indicated in Table 1. The results of this procedure are shown in Fig. 10 where the non-linearity of PID controller

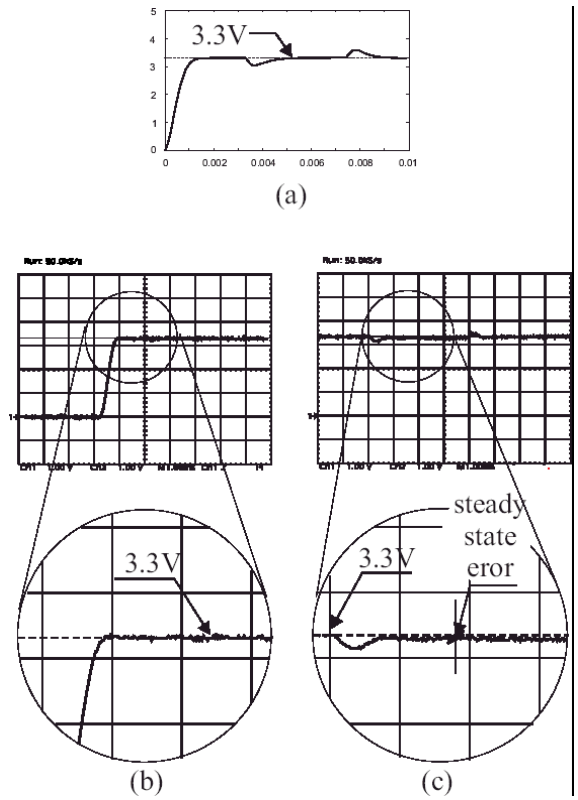

Figure 11: The output voltage u_0 response (the decomposed fuzzy PID controller). (a) Matlab-Simulink simulation of decomposed fuzzy PID controlled buck converter, start-up and load change response; experimental step response of a decomposed fuzzy PID controller(b) and the change of load from 6.8 to 4.8 Ω (c).

gains N_p, N_i, and N_d are shown. These gain characteristics were assigned by Matlab and afterwards written in a look-up table and implemented on the micro-controller unit. The decomposed PID structure implemented in DSP unit is shown in Fig. 8. The algorithm is investigated by simulation and verified by experiment. The result of simulation (the output voltage response) is shown in Fig. 11a. The experimental result showing the step response for a decomposed fuzzy PID controller tuned for a closed loop system with a state controller are given in Fig. 11b and c. There is no

K_I
(1) if e(k)=NB then y=NB
(2) if e(k)=NS then y=NS
(3) if e(k)=ZE then y=ZE
(4) if e(k)=PS then y=PS
(5) if e(k)=PB then y=PB

Table 1: N_I Fuzzy rules.

overshoot at the start-up, but the steady state is still noticed when the load resistance is changed. The over and under-shoot of the output voltage at the load change was 470 mV peak-to-peak (Vpp), which is the same as in the case when only the state controller has been used, but the steady state error was decreased to 39 mV. The settling time of the step response was 1ms, and the settling time at the load resistance change was 600μs. So organized control rules were solved by using the above mentioned DSP processor. In order to improve the over and under-shoot dynamics, the fuzzy state space controller shown in Fig. 12 was investigated.

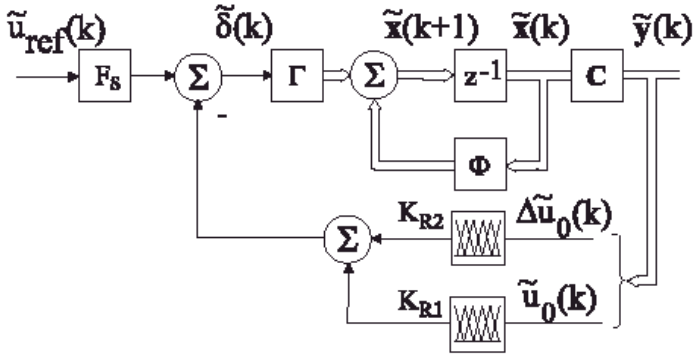

Figure 12: The fuzzy state controller scheme.

2.3 Fuzzy state space controller

To reduce the overshoot and steady state error the structure of the space controller shown in Fig. 12 has been proposed. The DSP implementation is shown in Fig. 13. In the structure of the state space controller a nonlinearity

gains were used instead of a constant value of state controller gains $\mathbf{K}_R$ (Fig. 4). To define this nonlinearity a fuzzy system is used.

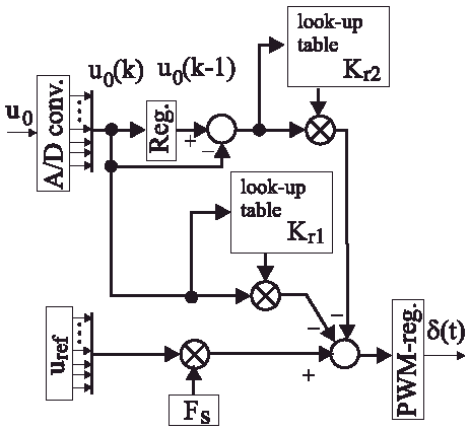

Figure 13: The fuzzy state controller scheme (DSP implementation).

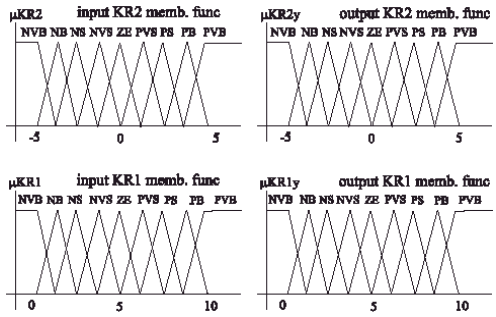

Figure 14: Membership functions for K_{R2} and K_{R1} fuzzy systems.

Two fuzzy systems were designed. The first one is used to adjust the controller gain responsible for the derivative of the output voltage control (K_{R2}), and the second one is used to adjust the controller gain responsible for the output voltage control (K_{R1}). One input/output system was used for each fuzzy system. Nine membership functions were used for each input/output to achieve fine decision mode. The position of membership functions was defined experimentally. Membership functions are shown in Fig. 14. Fuzzy rules were also designed experimentally for each system. For

the fuzzy state space controller, the gains K_{R2} and K_{R1} are evaluated by using the membership function shown in Fig. 14 and the linguistic description described in Tables 2 and 3. The non-linearities presented with fuzzy systems K_{R2} and K_{R1} are shown in Fig. 15. This gain characteristics were written in the look-up table, as shown in Fig. 13.

K_{R2}
if KR2(k)=NVB then KR2y=NVB
if KR2(k)=NBS then KR2y=NVB
if KR2(k)=NS then KR2y=NVB
if KR2(k)=NVS then KR2y=NVS
if KR2(k)=ZE then KR2y=ZE
if KR2(k)=PVS then KR2y=PVS
if KR2(k)=PS then KR2y=PS
if KR2(k)=PB then KR2y=PB
if KR2(k)=PVB then KR2y=PVB

Table 2: K_{R2} fuzzy rules.

K_{R1}
if KR1(k)=NVB then KR1y=NVB
if KR1(k)=NBS then KR1y=NB
if KR1(k)=NS then KR1y=NS
if KR1(k)=NVS then KR1y=NVS
if KR1(k)=ZE then KR1y=ZE
if KR1(k)=PVS then KR1y=PVS
if KR1(k)=PS then KR1y=PS
if KR1(k)=PB then KR1y=PB
if KR1(k)=PVB then KR1y=PVB

Table 3: K_{R1} fuzzy rules.

This control laws were investigated by Matlab simulation and verified by experiment. Fig. 16a shows the simulation result. Figs. 16b and 16c show the experimental results. From Fig. 16b, one can notice that the settling time of the step response is 0.8 ms. Fig. 16c shows that the output voltage overshoot caused by changing the load resistance has settling time 0.3 ms and the overshoot peak to peak is 260 mV. The static error was 11 mV.

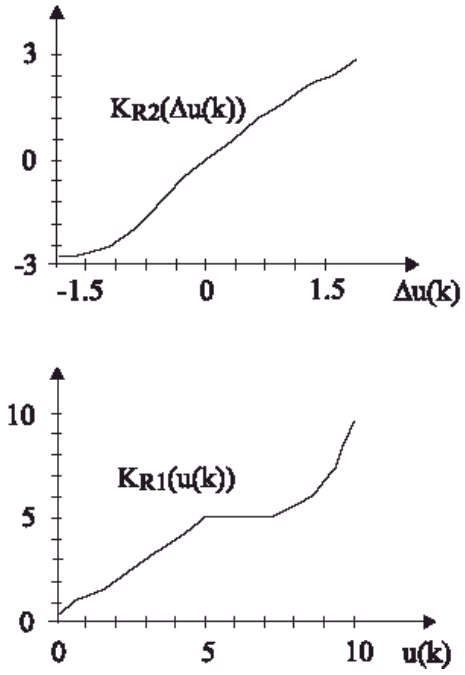

Figure 15: Nonlinearities presented using fuzzy systems K_{R2} and K_{R1}.

2.4 Discussion of results

The quantitative assessment based on the measured output converter voltage, was performed. The dynamic error e_d was evaluated as:

$$e_d = \max |u_{ref} - u_0|.$$

The steady state error e_s was measured after the transient (after settling time t_{set}) as the difference between the voltage reference and the output voltage:

$$e_s = u_{ref} - u_0.$$

The integrated quadratic error was evaluated by:

$$e_{int.} = \int_{t_1}^{t_{set}} (u_{ref} - u_0)^2 dt$$

where t_1 is the moment when the load change appears. The results of assessments for all three experiments were summarized in Table 4. According to these results, the best choice is the Fuzzy state controller.

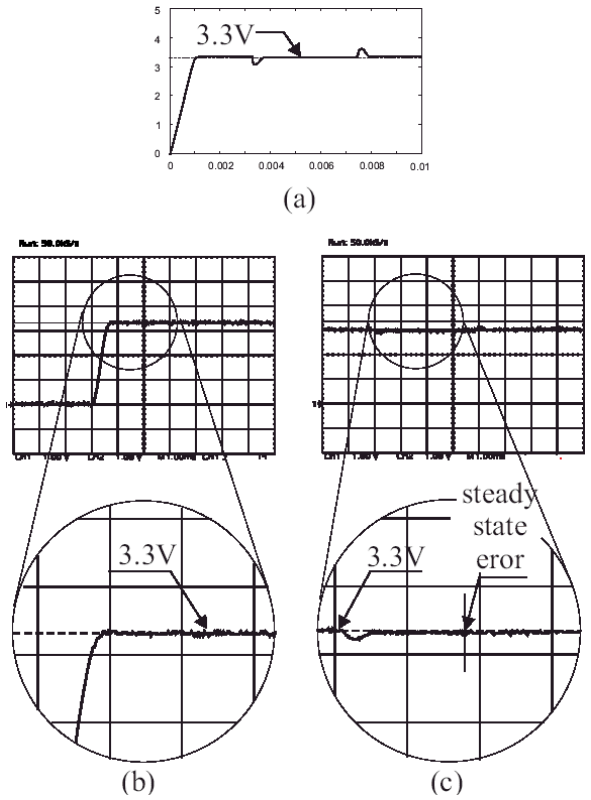

Figure 16: The fuzzy state space controller response. (a) Matlab-Simulink simulation of state space controlled buck converter, start-up, and load change response; experimentally measured the step response of a fuzzy state controller(b) and the change of load from 6.8 to 4.8 Ω (c).

	e_d	e_s	$e_{int.}$
State control.	$\pm 255\ mV$	$78\ mV$	$20.3 \times 10^{-6}\ V^2 s$
Decom. PID contrl.	$\pm 235\ mV$	$39\ mV$	$14.8 \times 10^{-6}\ V^2 s$
Fuzzy state contrl.	$\pm 133\ mV$	$11\ mV$	$4.07 \times 10^{-6}\ V^2 s$

Table 4: Resume of measurements.

3 Conclusion

Digital nonlinear algorithms using fuzzy logic were studied in order to control buck converter output voltage. The state controller, the state controller supported by decomposed fuzzy PID algorithm, and the fuzzy state controller were presented. Both decomposed fuzzy PID and fuzzy state controllers were supported by fuzzy algorithm in order to adapt the PID and state controller gains to the nonlinearity caused by changing of the converter load resistance. All algorithms were implemented on the 16-bit RISC microcomputer. The results were measured using markers on digital oscilloscope and using data acquisition tools of EXCEL. A decomposed fuzzy discrete PID controller demonstrates almost the same overshoots as the ordinary state controller. The best step response is achieved by the fuzzy state space controller, which is able to eliminate overshoots faster and achieves the smallest overshoot among all presented controllers. The main goal for digitalization of different control algorithms was a feasibility study for FPGA implementation of chosen controllers. According to this, the fuzzy state space controller can be easy implemented by FPGA circuit.

References

[1] R.D. Middlebrook and S. Cuk, IEEE Power Electronics Specialists Conference, PESC'76, p.19 (1976).

[2] V.I. Utkin, IEEE Trans. on Automatic Control **22**, 212 (1977).

[3] A. de Castro, P. Zumel, O. Garcia, T. Riesgo, and J. Uceda, IEEE Trans. on Power Electronic **18**, 334 (2003).

[4] W-C. So, C.K. Tse, and Y-S. Lee, IEEE Trans. on Power Electronics **11**, 24 (1996).

[5] M. Golob and B. Tovornik, ISA Transactions **42**, 89 (2003).